Empirical Force Field Calculations. 10. Conformational Analysis of *cis*-Decalin[1]

Jan M. A. Baas,*[2a] Bastiaan van de Graaf,[2a] Dirk Tavernier,[2b] and Paul Vanhee[2b]

Contribution from Laboratory of Organic Chemistry, Delft University of Technology, Julianalaan 136, 2628 BL Delft, The Netherlands, and the Department of Organic Chemistry, State University of Gent, Krijgslaan 271 (S4bis), B-9000 Gent, Belgium.
Received October 30, 1980

Abstract: Molecular mechanics was applied to the conformational analysis of *cis*-decalin: chair–chair (CC), chair–twist (CT), and twist–twist (TT) forms were calculated. The pseudorotation in the CT and TT manifolds was explored. In the TT manifold two distinct pseudorotating families of different symmetry (C_2 and C_1) were found. Some CT and TT forms are intermediates of the CC to inverted CC interconversion. The barrier to ring inversion in *cis*-decalin is calculated to be the CT to TT transition state and amounts to 12.0 kcal mol^{-1} (experimental value 12.4 kcal mol^{-1}). The geometry of this transition state is compared with literature proposals.

Accurate experimental data are available for the chair–chair to chair–chair flipping of *cis*-decalin (*cis*-decahydronaphthalene):[3] $\Delta H^{\ddagger}$ = 12.4 kcal mol^{-1}, $\Delta S^{\ddagger}$ = 0.1 cal K^{-1} mol^{-1}. The precise mechanism of this conformational process is not known, but two proposals have been made. These are outlined in Figure 1. First one of the *cis*-decalin rings, say ring A,[4] assumes a twist con-

formation by inverting the endocyclic torsion angles of its peripheral bonds.[5] Gerig and Roberts[6] have proposed that in a second and rate-determining step ring B would convert to a twist form, also "along" its peripheral bonds. The twist–twist conformation now pseudorotates to the enantiomeric form. The inverted chair–chair is then attained by two consecutive twist-to-chair transformations, palindromically symmetric with the above described ones. De Pessemier, Anteunis, and Tavernier[7] have envisaged a different rate-determining step: ring B would convert to a twist conformation along the central bond. They argued that such an "open" transition state, with eclipsed bonds around 9–10, should relieve much of the nonbonded strain present in the crowded, concave side of the chair–chair ground state. Neither of these two proposals has had the benefit of verification by a molecular-mechanics calculation with good minimization and a reliable force field. Such a study is the subject of the present paper.

Specification of a Conformation of *cis*-Decalin

We shall describe a geometry of *cis*-decalin by (i) specifying the inter-ring relation and (ii) stating the conformation of each ring. The inter-ring relation concerns the geometry at the ring fusion. It is expressed qualitatively by showing the angular hydrogen atoms above or below some usually loosely defined reference plane. It can be specified quantitatively with the signed values of the torsion angles around the central bond (Figure 2). As we are primarily concerned with the internal coordinates of the carbon skeleton, we shall specify the values of three carbon-carbon torsion angles around this bond; the value of the fourth is fixed then. The inter-ring relation can be stated in other but equivalent ways. For instance, one might specify the values of the endocyclic torsion angles around the central bond along with the value of one of the projected exocyclic valency angles in Figure 2.[8] Note that the cis fusion imposes a constraint: the endocyclic torsion angles around the central bond have the same sign and about the same magnitude in both rings.

We now pay attention to the conformations of the separate six-membered rings of *cis*-decalin. There are two species of cyclohexane conformations: the rigid chair (C) forms of D_{3d} symmetry and the flexible conformational manifold (T) characterized by a twofold rotation axis perpendicular to the mean plane of the ring.[10,11] Rigid means that the ring torsion angles cannot be changed without a simultaneous change of the valency angles; the adjective flexible refers to an internal degree of freedom: the torsion angles change concertedly while one and only one of them varies at will between the limiting values $+\theta_{max}$ and $-\theta_{max}$. The conformational changes brought about by varying the torsion angles are described as pseudorotation. On the pseudorotation circuit the familiar boat (B) and D_2 twist (D_2T) forms[12] are

(1) Preceding papers, part VIII: van de Graaf, B.; Baas, J. M. A.; Widya, H. C. *Recl. Trav. Chim. Pays-Bas* **1981**, *100*, 59–61. Part IX: Peters-van Cranenburgh, P. E. J.; Peters, J. A.; Baas, J. M. A.; van de Graaf, B.; de Jong, G. *Ibid.* **1981**, *100*, 165–168.

(2) (a) Delft University. (b) Gent University.

(3) Mann, B. E. *J. Magn. Reson.* **1976**, *21*, 17–23.

(4) *cis*-Decalin has a twofold rotation axis perpendicular to the bond 9–10. Rings A and B are therefore symmetrically equivalent. Note also that a chair–chair *cis*-decalin and its inverted chair–chair partner are enantiomers. The ring inversion is simultaneously a racemization process.

(5) There are four kinds of constitutionally nonequivalent C–C bonds: central (9–10), inner (1–9, 8–9, 4–10, 5–10), outer (1–2, 3–4, 5–6, 7–8), and exterior (2–3, 6–7). The outer and exterior bonds together are called peripheral bonds. We look at *cis*-decalin as made up of two six-membered rings. Therefore an endocyclic valency angle is one whose three atoms are part of the same six-membered ring, e.g., 8–9–10, whereas in an exocyclic valency angle the three atoms are contained in different rings, e.g., 8–9–1. Similarly, an endocyclic torsion angle is subtended by three bonds (or four atoms) of the same ring, e.g., 1–9–10–4, and in an exocyclic torsion angle the constituent bonds belong to different rings, e.g., 4–10–9–8. There are two exocyclic valency angles and six exocyclic torsion angles.

(6) Gerig, J. T.; Roberts, J. D. *J. Am. Chem. Soc.* **1966**, *88*, 2791–2799. Contrary to the caption, Figure 3 of this paper depicts in our opinion a possible transition state between the chair–twist and twist–twist forms.

(7) De Pessemier, F.; Anteunis, M.; Tavernier, D. *Bull. Soc. Chim. Belg.* **1978**, *87*, 179–187.

(8) Geise and co-workers[9] have expressed the inter-ring relation by a "connection angle" which is the dihedral angle between two planes, one of which bisects the torsion angle 1–9–10–4 and the other one 8–9–10–5. If the values of these torsion angles are the same, the values of the connection angle and the projected exocyclic valency angles are also equal. In a general case, where the endocyclic torsion angles are different from each other, the connection angle is a function of the exocyclic valency angle and the endocyclic torsion angles.

(9) Van Den Enden, L.; Geise, H. J.; Spelbos, A. *J. Mol. Struct.* **1978**, *44*, 177–185.

(10) Hazebroek, P.; Oosterhoff, L. J. *Discuss. Faraday Soc.* **1951**, *10*, 87–93.

(11) Dunitz, D. J.; Waser, J. *J. Am. Chem. Soc.* **1972**, *94*, 5645–5650.

(12) The word "boat" (B) is always linked with the C_{2v} form of the pseudorotation circuit, but there is no generally accepted name to distinguish the D_2 twist from the general C_2 flexible form. In fact, the IUPAC committee on nomenclature (Section E: Stereochemistry (Recommendations 1974), rule E-5.2.c) terms a twist conformation "a median conformation through which one boat form passes during conversion into the other boat form". We will use twist for any form on the pseudorotation path and D_2 twist whenever that particular geometry is meant.

0002-7863/81/1503-5014$01.25/0

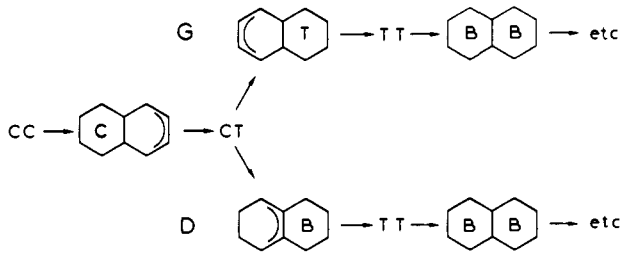

Figure 1. Outline of the proposed transition states in the inversion of *cis*-decalin from chair–chair (CC) via chair–twist (CT) and twist–twist (TT) to the inverted series. B denotes a boat form and the arcs denote four atoms in the same plane. G refers to the proposal of Gerig and Roberts[6] and D to that of De Pessemier, Anteunis, and Tavernier.[7]

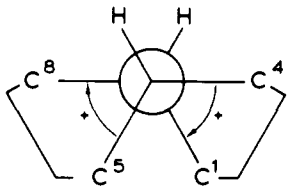

Figure 2. Newman projection of the central bond.

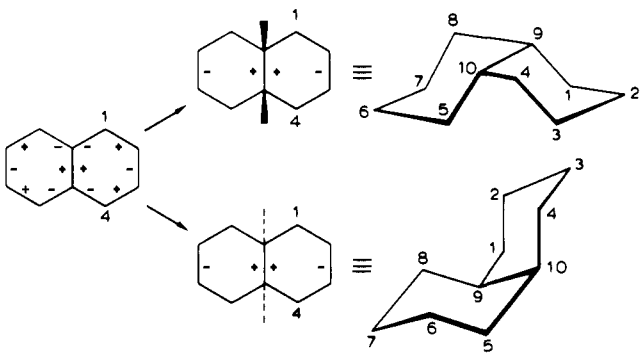

Figure 3. Two differently numbered chair–chair *cis*-decalins.

encountered. In *cis*-decalin the two six-membered rings can assume the same conformation (chair or twist), or one ring can be in the chair and the other in the twist conformation. These forms are denoted CC, TT, and CT or TC, respectively.

Geometric Considerations

Before the presentation of a quantitative description of the potential-energy surface with the use of molecular mechanics, we pay attention to the geometries of *cis*-decalin on the basis of idealized framework models with undeformable bond lengths and valency angles.

Chair–Chair Conformation. The CC forms of *cis*-decalin are specified by the sign and the magnitude of the two endocyclic torsion angles around the central bond along with that of one of the exocyclic torsion angles. In the sequel we need atom numbers to specify internal coordinates. In the numbering of CC *cis*-decalin we must choose which of the four constitutionally equivalent carbon atoms will be given the number 1. Dependent on this choice two different series of *numbered cis*-decalins can be obtained. For instance, in the upper formula of Figure 3 the atoms 4 and 8 are anti, and in the lower one they are gauche related. These two series of numbered *cis*-decalins cannot be interconverted by conformational processes; each structure yields the mirror image of the other one after inversion.

At this point, we choose the numbering in such a way that the exocyclic torsion angle 8–9–10–4 varies between anti and +gauche in the process of inversion from the CC form with positively signed endocyclic torsion angles around the central bond to that with negatively signed ones.

Twist–Twist Manifold. The description of the TT conformations is much more involved, because of the pseudorotation freedom. In twist cyclohexane the choice of the torsion angle around say

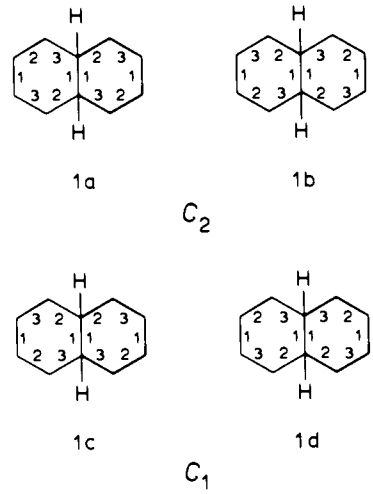

Figure 4. C_1 and C_2 conformations of TT *cis*-decalin. Only the subscripts of the three principally distinct torsion angles θ_1, θ_2, and θ_3 are shown.

1–2 at a value θ_1 simultaneously fixes the symmetry independent torsion angles at the values θ_2 and θ_3. One can place θ_2 around 2–3 and θ_3 around 3–4 or the other way round. This is not due to an extra degree of freedom, but results from the numbering itself, which makes distinguishable what was previously undistinguishable. Indeed, either choice gives precisely the same conformation of twist cyclohexane, as it must do, because with the selection of θ_1 the one and only freely assignable torsion angle was spent. In the TT conformations of *cis*-decalin we may select any endocyclic torsion angle, say along the central bond, as the freely assignable internal coordinate; this simultaneously fixes the torsion angle along the central bond in the second ring. Even so, the TT conformation is not completely specified. As discussed above, there are in each ring two ways to place the remaining torsion angles and thus four possibilities for the numbered TT bicyclic system as a whole. These four possibilities are shown in Figure 4, where for brevity the torsion angles are denoted as 1, 2, and 3. The geometries expressed by these four sets of torsion angles are not identical. The forms **1a** and **1b** have a twofold rotation axis, while **1c** and **1d** are devoid of symmetry. Forms **1a** and **1b** are distinct, but **1c** and **1d** are superimposable. Three torsion angles are thus needed to describe a flexible conformation of *cis*-decalin. As the torsion angles around the central bond can vary concertedly between $+\theta_{max}$ and $-\theta_{max}$, the analysis of Figure 4 foreshadows the existence of two different pseudorotation paths in flexible *cis*-decalin: the C_2 path on which the conformers have a twofold rotation axis and the C_1 path on which the pseudorotation partners have in general no symmetry.[13] These symmetric and asymmetric paths might also be named the "pseudoconrotameric" and "pseudodisrotameric" circuits, respectively, as has been used in bicyclo[3.3.0]octane systems.[15] On each path six BB and six D_2T–D_2T forms are encountered while the torsion angles run through their gamut of values. These forms are shown schematically in Figure 5. The inter-ring relation is expressed qualitatively by the "up" angular hydrogen atoms in the upper conformations. A perspective view of the BB forms is also given. On both paths the structures above and below the horizontal axis of the drawing are enantiomers; the structures on the horizontal line are achiral. On the C_2 path, there are con-

(13) Dunitz[14] has shown that the existence of the D_{3d} (chair) and C_2 (twist) forms of an equilateral and equiangular six-membered ring can be deduced by expressing the same carbon–carbon distances in terms of different internal coordinates, e.g., d_{1-4}, the distance between atoms 1 and 4, by internal coordinates along 1–2–3–4 and 1–6–5–4, respectively. Similarly, the existence of CC, CT(TC), and C_2- and C_1-TT conformations of *cis*-decalin can also be demonstrated by expressing d_{1-4} in internal coordinates along 1–2–3–4 and 1–9–10–4, d_{5-8} in those along 5–10–9–8 and 5–6–7–8, and d_{9-10} in those along 9–1–2–3–4–10 and 9–8–7–6–5–10.

(14) Dunitz, D. J. *J. Chem. Educ.* **1970**, *47*, 488–490.

(15) Anteunis, M.; Verhegghe, G.; Rosseel, T. *Org. Magn. Reson.* **1971**, *3*, 693–701.

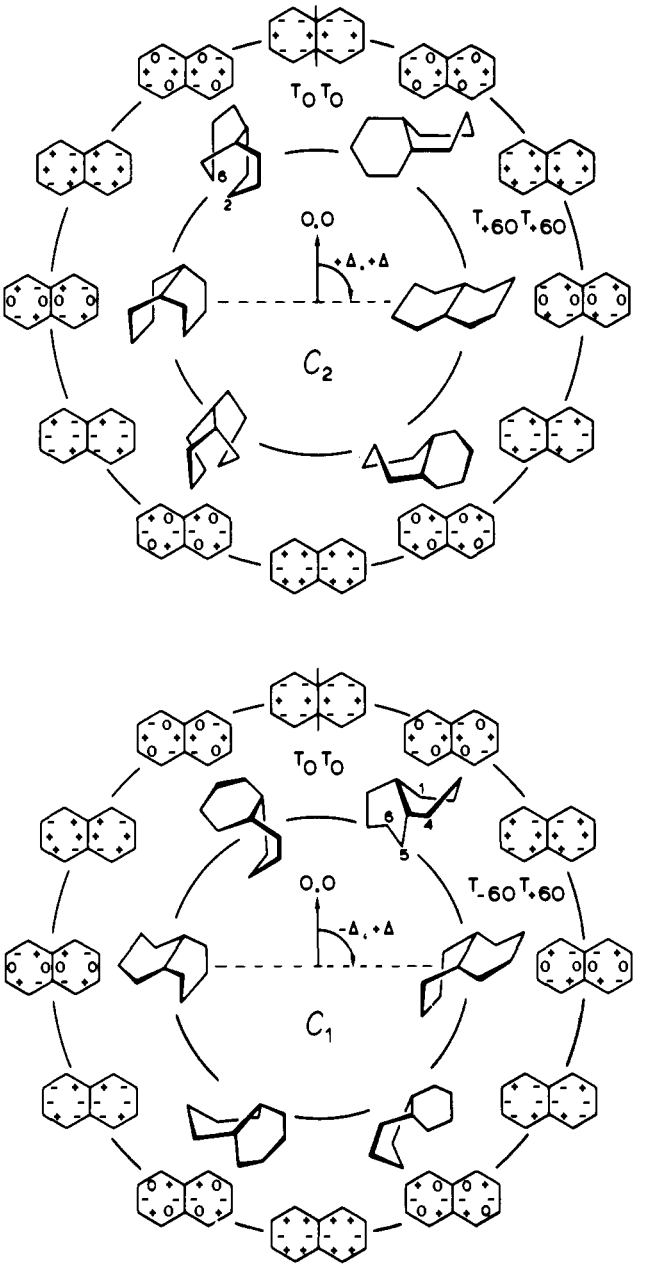

Figure 5. The C_1 and C_2 pseudorotation paths in TT *cis*-decalin with a perspective view of the boat-boat forms encountered on these paths.

spicuous geometric differences between the left-hand and right-hand side of the figure. In the W-shaped structure at right the interactions between the two rings seem small. At left there is a compact, cage-like arrangement. This is not so on the C_1 path. Here the structures at left and right are identical, including the chirality (homomeric forms, homomers). Their geometry looks like a blend of the corresponding right- and left-hand side conformations of the C_2 path. The C_1 and C_2 pseudorotation paths have two enantiomeric structures in common, the uppermost and the lowermost ones of each cycle. This happens, as is seen from Figure 4, because incidentally θ_2 equals θ_3. The passage from one path to the other is possible by way of these geometries.

We now discuss the application of the cyclohexane pseudorotation equation 1 to TT *cis*-decalin. In eq 1 θ_j is the jth ring torsion

$$\theta_j = \theta_{max} \cos [\Delta + (2\pi/3)(j - 1)] \quad (1)$$

angle (j takes the values 1–6 and Δ runs between $-\pi$ and $+\pi$). This relation was proved by Dunitz[16] in the case of an infinitesimally puckered regular hexagon and was experimentally shown

(16) Dunitz, D. J. *Tetrahedron* **1972**, *28*, 5459–5467.

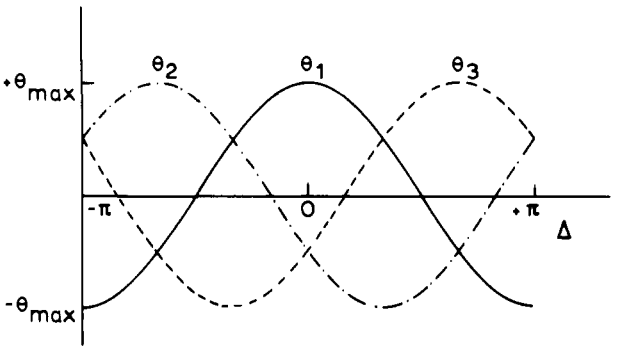

Figure 6. Plot of θ_1, θ_2, and θ_3 as a function of Δ and θ_{max} during pseudorotation.

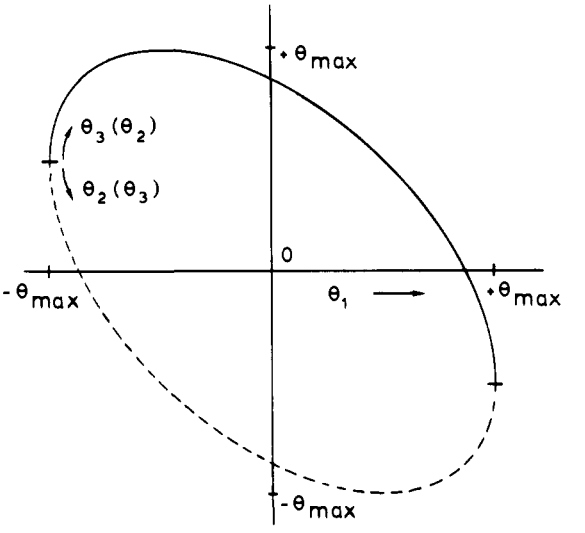

Figure 7. Plot of θ_2 and θ_3 as a function of θ_1 during pseudorotation. θ_2 and θ_3 are given by the full and the broken line of the ellipse or the other way round.

by Buys and Geise[17] to be a very good approximation for puckered six-membered rings. Equation 1 expresses the torsion angles as a function of the independent variables θ_{max} and Δ, which are therefore called puckering coordinates. θ_{max} is related to the endocyclic valency angle,[18] and the phase angle of pseudorotation Δ is a mathematical variable. Figure 6 shows θ_1, θ_2, and θ_3 (coincident with, respectively, θ_4, θ_5, and θ_6) as a function of θ_{max} and Δ. Equation 1 can be transformed so that θ_2 and θ_3 are expressed as a function of θ_{max} and θ_1. A graph of these functions is given in Figure 7.

$$2\theta_2 = -\theta_1 \pm [3(\theta_{max}^2 - \theta_1^2)]^{1/2} \quad (2a)$$

$$2\theta_3 = -\theta_1 \mp [3(\theta_{max}^2 - \theta_1^2)]^{1/2} \quad (2b)$$

For *cis*-decalin we number the bonds of the rings A and B clockwise, starting from the central bond which has number 1.

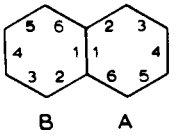

The torsion angles of ring A are given by eq 3a. The torsion

$$\theta_j^A = \theta_{max} \cos [\Delta + (2\pi/3)(j - 1)] \quad (3a)$$

(17) Buys, H. R.; Geise, H. J. *Tetrahedron Lett.* **1968**, 5619–5624.

(18) For infinitesimally small puckering $\theta_{max}^2 = 16(2\pi/3 - \beta)/\sqrt{3}$[16] where β is the endocyclic valency angle. For the tetrahedral valency angle θ_{max} is calculated at 74.65°, whereas the exact value is 70.67° (numerical calculation due to: Bottomley, G. A.; Jefferies, P. R. *Aust. J. Chem.* **1961**, *14*, 657–660).

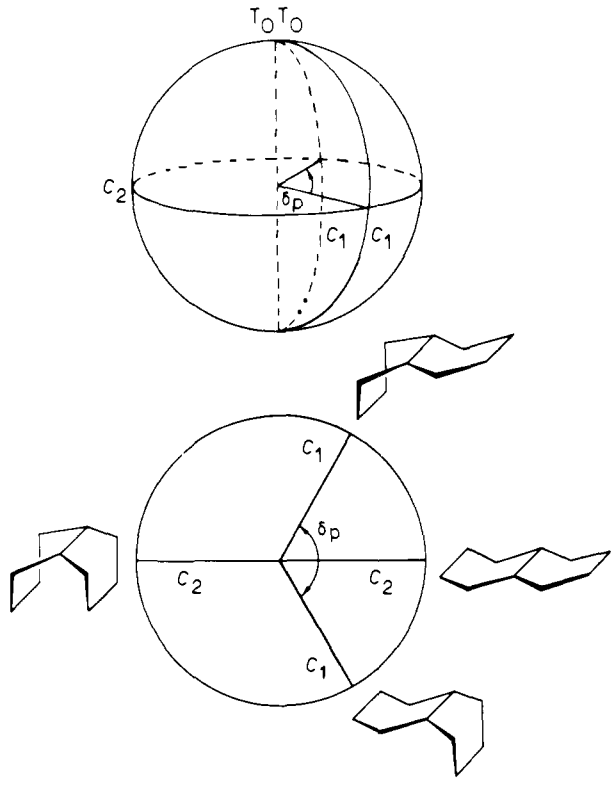

Figure 8. Representation of the C_1 and C_2 paths on a sphere and the projection of the equatorial plane.

angles of ring B are different on the C_2 and the C_1 path and are expressed by eq 3b and 3c, respectively. The exocyclic torsion

$$\theta_j^{B,C_2} = \theta_{max} \cos [\Delta + (2\pi/3)(j-1)] \quad (3b)$$

$$\theta_j^{B,C_1} = \theta_{max} \cos [-\Delta + (2\pi/3)(j-1)] \quad (3c)$$

angles along the central bond, defined by the atoms 8–9–10–4 and 1–9–10–5, are given by eq 3d and 3e, wherein δ_p is the absolute

$$\theta_{8-9-10-4} = +\delta_p + \theta_{max} \cos \Delta \quad (3d)$$

$$\theta_{1-9-10-5} = -\delta_p + \theta_{max} \cos \Delta \quad (3e)$$

value of the projected exocyclic valency angle (Figure 2, angle 4–10–5). The variable δ_p arises naturally as a third puckering coordinate. The positive sign of δ_p used in eq 3d (and the negative sign in eq 3e) reflects our earlier choice with respect to the numbering of *cis*-decalin. The remaining exocyclic torsion angles are a function of the already defined valency angles and Δ. The set of equations 3 suggests the representation of the pseudorotation in TT *cis*-decalin on a sphere (Figure 8). The radius of the sphere is proportional to θ_{max}. The azimuthal angle represents δ_p. Two halves of great circles meeting at the poles and enclosing δ_p represent the C_1 path; on one half-circle Δ is negative, and on the other one Δ is positive. The C_2 circuit is symbolized by a great circle which bisects δ_p such that say the positive Δ region is enclosed by the C_1 half-circles. The equator splits the sphere into enantiomeric hemispheres, and in Figure 8 the equatorial plane is shown. The structures at the south and north pole are the enantiomeric conformations common to the C_1 and C_2 paths. It is a merit of this spherical representation that it accurately reflects that the positive and negative Δ parts of the C_2 path are different.[19] The spherical representation of the puckering coordinates (Figure 8) and the cycles of Figure 5 can be related by equating the angular coordinate in Figure 5 with Δ, zero on the vertical axis and $+\pi/2$ or $-\pi/2$ on the horizontal axis at right and left, respectively.

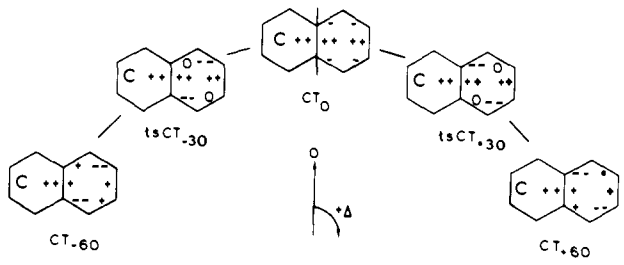

Figure 9. The nonideal pseudorotation in chair–twist *cis*-decalin.

For a denomination of the various TT conformations, a notation with θ_{max}, δ_p, C_2, and Δ could be used. Once defined, θ_{max} and δ_p remain constant and may be omitted. We treat then the rings A and B separately, determining their phase angle according to eq 1 on the basis of the numbering used in eq 3. There result notations $T_{+\Delta}T_{+\Delta}$ and $T_{-\Delta}T_{+\Delta}$ for the C_2 and C_1 path, respectively. The symbols are ordered ring B–ring A. The computed geometries of the TT conformations will be denominated by the label of the ideal form to which they are intuitively similar.

Chair–Twist Forms. In the CT conformation the rigid chair form fixes the central torsion angle on the twist side near θ_{max}. Therefore the whole CT form is, strictly speaking, rigid. Small changes of the central torsion angle allow much larger changes in the adjacent angles of the twist form (see Figures 6 and, particularly, 7). Slight deformations should therefore make possible a limited "nonideal" pseudorotation of the CT form. Indeed, the manipulation of framework models shows that the twisted ring can be rotated to adjoining boat forms and beyond without noticeable resistance. This limited pseudorotation is shown in Figure 9. For emphasis of its nonideality, the large torsion angles near θ_{max} are signed twice and angles near half-θ_{max} only once. This figure is at the basis of the labels given to the computed conformations.

Computational Results

As in earlier studies the Engler force field[20] was used with the Delft molecular-mechanics program.[21] The conformational energy, the point group, the endocyclic torsion angles, and one exocyclic torsion angle of the stable conformations and the transition states are shown in Table I for one of the enantiomeric halves of the conformational space. Cartesian coordinates and lists of all bond lengths, valency angles, and torsion angles of all structures will be sent upon request. The stable conformations are labeled with capital letters. The transition states are identified by the lower case letters ts.

Chair–Chair Conformer. The geometry of CC *cis*-decalin as calculated here agrees well with electron diffraction data and calculations[9] using the force field of Lifson and Warshel[22] and Boyd,[23] especially with the latter one. The present structure is a little flatter (mean $\theta = 53.7°$) than that calculated with the Boyd force field (mean $\theta = 54.2°$). The central torsion angle and the inner torsion angles involving equatorial bonds (4–10 and 8–9) are smaller than in cyclohexane, whereas the inner torsion angles involving axial bonds (1–9 and 5–10) are larger and have almost the cyclohexane and peripheral torsion angle value. This is the result of unfavorable interactions between the axial methylenes and the syn-axial hydrogen atoms.

Chair–Twist Family. The pseudorotation path is computationally studied by driving the mean of three torsion angles around 1–9. This mapping parameter is stepped by 5° and then con-

(19) In our idealized model of *cis*-decalin both the endocyclic and the exocyclic valency angles have the same tetrahedral value. This is of an accidental nature. Conceptually, these valency angles have different effects on the conformational description of [4.4.0] bicyclic systems. We have not been able to dream up a chemical example of a [4.4.0] system with identical endocyclic valency angles, numerically different from the exocyclic valency angles. One can, however, construct mechanical models, e.g., with endocyclic valency angles of 90° and exocyclic valency angles of 180°. One sees then that the positive and negative parts of the C_2 path become identical, as the spherical representation of the puckering coordinates immediately suggests.

(20) Engler, E. M.; Andose, J. D.; Schleyer, P. von R. *J. Am. Chem. Soc.* **1973**, *95*, 8005–8025.
(21) Van de Graaf, B.; Baas, J. M. A.; van Veen, A. *Recl. Trav. Chim. Pays-Bas* **1980**, *99*, 175–178.
(22) Lifson, S.; Warshel, A. *J. Chem. Phys.* **1968**, *49*, 5116–5129.
(23) Chang, S.; McNally, D.; Shary-Tehrany, S.; Hickey, M. J.; Boyd, R. H. *J. Am. Chem. Soc.* **1970**, *92*, 3109–3118.

Table I. Computational Results for *cis*-Decalin with the Engler Force Field

conformation[a]	point group	energy[b]	n[d]	torsion angles,[e] deg: ring A 1-2	2-3	3-4	4-10	10-9	9-1	ring B 5-6	6-7	7-8	8-9	9-10	10-5	4-10-9-8
CC	C_2	0.0[c]	0	56	−55	54	−51	51	−54	56	−55	54	−51	51	−54	179
CT_{-60}	C_1	8.0	0	−53	29	27	−61	36	19	53	−60	59	−49	41	−44	168
ts CT_{-30}	C_1	8.5	1	−45	43	4	−49	46	0	54	−58	58	−51	47	−49	176
CT_0	C_1	5.8	0	−20	61	−45	−10	52	−36	57	−54	52	−52	53	−56	180
ts CT_{+30}	C_1	5.9	1	−6	55	−52	1	48	−46	57	−55	53	−51	51	−55	177
CT_{+60}	C_1	5.3	0	25	34	−59	21	39	−64	57	−59	55	−47	44	−49	168
ts[CT↔CT]1	C_1	9.9	1	−13	1	37	−64	51	−14	57	−55	54	−52	53	−56	180
ts[CC↔CT]2	C_1	9.8	1	50	−11	−11	−7	46	−69	56	−57	56	−51	48	−51	174
ts $T_{-90}T_{-90}$	C_{2v}	14.1	1	−47	0	47	−47	0	47	−47	0	47	−47	0	47	131
$T_{-60}T_{-60}$	C_2	13.3	0	−52	12	41	−55	15	38	−52	12	41	−55	15	38	145
ts $T_{-30}T_{-30}$	C_2	16.5	1	−43	27	24	−59	42	7	−43	27	24	−59	42	7	173
T_0T_0	C_2	11.4	0	−20	59	−39	−18	57	−37	−20	59	−39	−18	57	−37	175
ts $T_{+30}T_{+30}$	C_2	11.8	1	−6	55	−50	−2	51	−46	−6	55	−50	−2	51	−46	178
$T_{+60}T_{+60}$	C_2	7.3	0	34	25	−63	37	22	−60	34	25	−63	37	22	−60	148
ts $T_{+90}T_{+90}$	C_{2v}	8.1	1	52	0	−52	51	0	−51	52	0	−52	51	0	−51	126
ts $T_{-30}T_{+30}$	C_1	14.2	1	−35	66	−38	−18	49	−22	−50	39	14	−57	45	7	178
$T_{-60}T_{+60}$	C_1	9.0	0	35	24	−63	40	19	−58	−59	20	36	−57	18	38	146
ts $T_{-90}T_{+90}$	C_1h	9.8	1	52	0	−52	52	0	−52	−50	0	50	−50	0	50	127
ts[CT↔TT]1	C_1	13.7	1	−47	−7	55	−46	−7	55	61	−67	37	−1	−5	−26	124
ts[CT↔TT]2	C_1	15.5	1	−41	−12	59	−50	−3	49	8	−48	65	−38	−4	19	127
ts[CT↔TT]3	C_1	13.5	1	−62	18	38	−53	10	46	70	−47	7	11	11	−51	139
ts[CT↔TT]4	C_1	15.7	1	−57	29	29	−61	32	24	−14	−15	54	−63	33	5	162
ts[CT↔TT]5	C_1	15.8	1	−20	61	−43	−13	54	−36	37	1	−11	−17	56	−66	181
ts[CT↔TT]6	C_1	15.6	1	−21	58	−35	−22	60	−37	−4	12	17	−54	62	−33	188
ts[CT↔TT]7	C_1	12.0	1	39	18	−61	44	13	−56	70	−45	6	11	13	−53	141
ts[CT↔TT]8	C_1	12.8	1	64	−28	−32	61	−25	−35	22	−62	56	−11	−28	23	102
ts[CC↔TT]	C_2	16.1	2	70	−54	16	9	5	−44	70	−54	16	9	5	−44	137

[a] Conformers are labeled with capital letters (C = chair, T = twist). The twist forms are subscripted with the approximate value of Δ. Transition states are prefixed with the lower case letters ts. The order is such that pseudorotation paths can be followed easily. [b] Conformational energy in kcal mol^{-1}. [c] Steric energy: 11.94 kcal mol^{-1}. [d] n = number of imaginary vibration frequencies. [e] Endocyclic torsion angles are indicated by the central bond only.

strained using a stiff potential-energy function. We have discussed earlier that the mean of several torsion angles can be a better approximation of the reaction coordinate than any of the individual torsion angles.[21] The conformational energy vs. mapping parameter graph is shown in Figure 10. The considerable pseudorotation freedom is striking. There are three energy minima in which the twisted ring resembles a D_2 twist and two transition states with boat-like forms. At the edges of the graph the system develops toward TT conformations and the energy rises steeply. Surprisingly CT_0, which resembles most the ideal pseudorotation partner, is not the most stable form. Its geometry is twisted (positive Δ) toward the more stable CT_{+60} conformation, which is 5.3 kcal mol^{-1} above CC. This is somewhat less than the twist-chair energy difference in cyclohexane (5.7 kcal mol^{-1}) by the same force field.[21] The barrier between CT_0 and CT_{+60} is negligibly low (smaller than RT). The form CT_{-60} is of much higher energy (8.0 kcal mol^{-1}), probably due to the interaction between the C^2 and C^5 methylene groups. As to why the ideal-framework-model approach fails, the following points may be noted: (1) The ring in the chair conformation does not really keep its central torsion angle constant, for compared with CT_0 this angle is 9 and 12° smaller in CT_{+60} and CT_{-60}, respectively. (2) The calculations do not bear out the idea that the two rings should have the same value for their central torsion angles. Differences up to 5° are found (CT_{-60} and CT_{+60}), and the smaller angle is always in the twisted ring A.

Chair–Chair to Chair–Twist Interconversion. *cis*-Decalin has 11 C–C bonds, but only 6 nonequivalent ones in the C_2 symmetric CC form. The reaction path along each of these six bonds was explored. Inversion along 9–10 proceeds directly to the TT family and will be considered separately. By driving the torsion angles of the five remaining C–C bonds two transition states ts[CC↔CT]1 and 2 were obtained. Continuous paths were found by selecting proper mapping parameters. The geometry of these ts's is characterized by three consecutive small torsion angles along the bonds of 9–1–2–3 and 2–3–4–10, respectively. In this respect they are reminiscent of the C_2 cyclohexane transition state.[21] The conformational energies of the two ts's are practically the same, 9.8 kcal mol^{-1}, and only slightly lower (0.3 kcal mol^{-1}) than the lowest cyclohexane transition state.

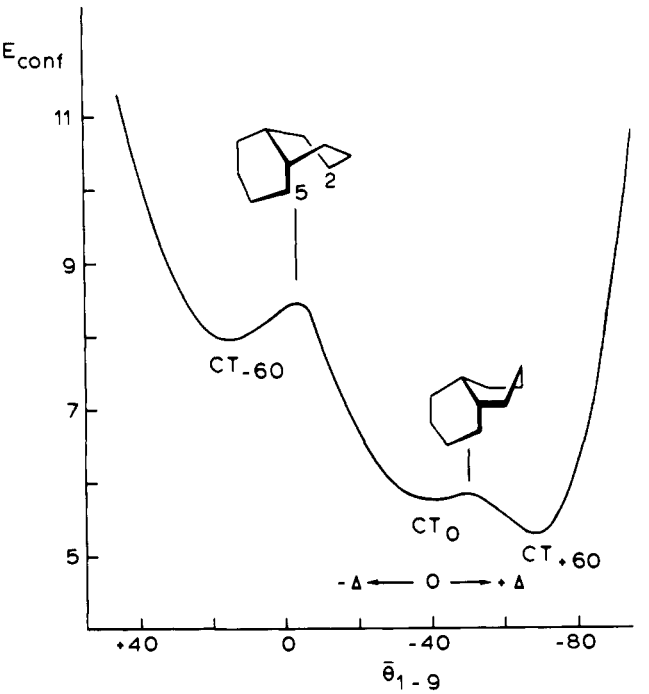

Figure 10. Conformational energy graph (kcal mol^{-1}) of pseudorotation in chair–twist *cis*-decalin. On the horizontal axis the mean of the driven torsion angles is set out and also approximate values of Δ.

Twist–Twist Family. We expect, on the basis of the ideal framework model, two distinct pseudorotation paths having C_2 and C_1 symmetric conformations, respectively. The computation fully confirms the expectation of a symmetric and nonsymmetric

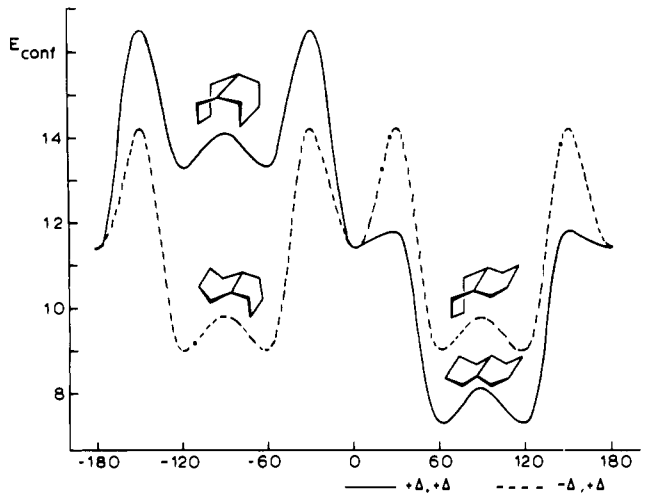

Figure 11. Conformational energy graph (kcal mol^{-1}) of pseudorotation in twist–twist *cis*-decalin. The broken line refers to the C_1 path and the full line to the C_2 path. On the horizontal axis approximate values of Δ are set out.

path. The graph of the conformational energy of the pseudorotation partners over the entire Δ range is shown in Figure 11. Continuous reaction paths between the stable conformations were again found by selecting proper mapping parameters for each interconversion. Figure 12 conveys at a glance the torsion angles of the stationary conformations of the TT family.

T_0T_0, the form common to the C_1 and the C_2 paths, has a conformational energy of 11.4 kcal mol^{-1}. The torsion angles of both rings in T_0T_0 are closely similar to those of the twisted ring in CT_0, and we also notice a close similarity between the pseudorotation around T_0T_0 on the symmetric path and around CT_0 in the chair–twist family. There is a very low barrier between T_0T_0 and $T_{+60}T_{+60}$, as there is between CT_0 and CT_{+60} (Figures 10 and 11).

The lowest energy TT form is $T_{+60}T_{+60}$ (7.3 kcal mol^{-1} above CC). The adjacent boat–boat transition state ts $T_{+90}T_{+90}$ to the enantiomer $T_{+120}T_{+120}$ lies but 0.8 kcal mol^{-1} higher. In these sterically unhindered conformations the ground-state strain of the cis fusion is absent. An estimate of this strain (2.7 kcal mol^{-1}) can be obtained from the experimental enthalpy difference between *cis*- and *trans*-decalin.[24] The conformational energies of $T_{+60}T_{+60}$ (7.3 kcal mol^{-1}) and ts $T_{+90}T_{+90}$ (8.1 kcal mol^{-1}) are less than two times the conformational energies of the corresponding cyclohexane forms D_2 twist (2 × 5.7 kcal mol^{-1}) and boat (2 × 6.7 kcal mol^{-1})[21] after accounting for the loss of ground-state strain imposed by the cis fusion. Indeed, the bicyclic system does not have twice the number of unfavorable interactions present in the isolated constituent rings. For instance, in ts $T_{+90}T_{+90}$ there are 9 eclipsed torsion angles (5 H–C–C–H and 4 C–C–C–C), whereas 2 boat cyclohexanes contain 12 eclipsed torsion angles (8 H–C–C–H and 4 C–C–C–C). An estimate of the conformational energy of ts $T_{+90}T_{+90}$ goes as follows: subtract the ethane barrier (3 eclipsed H–C–C–H torsion angles) and the strain of the cis fusion from twice the conformational energy of the boat form of cyclohexane (2 × 6.7 − 2.8 − 2.7 = 7.9 kcal mol^{-1}, in amazingly good agreement with the force field calculated value of 8.1 kcal mol^{-1}).

The stable conformations of highest energy are $T_{-60}T_{-60}$ and its enantiomer $T_{-120}T_{-120}$, with a conformational energy of 13.3 kcal mol^{-1}. They too are separated by a low barrier of 0.8 kcal mol^{-1}, and in the cage-like ts $T_{-90}T_{-90}$ the rings are but slightly flatter (4 or 5°) than in ts $T_{+90}T_{+90}$.

The high-energy transition states ts $T_{-30}T_{-30}$ and ts $T_{-30}T_{+30}$ are interesting. They have serious deviations from the ideal pseudorotation geometries and short distances between hydrogen atoms of the two rings. The opposite ring torsion angles differ by about 15° in both rings of ts $T_{-30}T_{-30}$ and in ring A of ts $T_{-30}T_{+30}$ (Figure 12). In ts $T_{-30}T_{-30}$ we find a very short distance

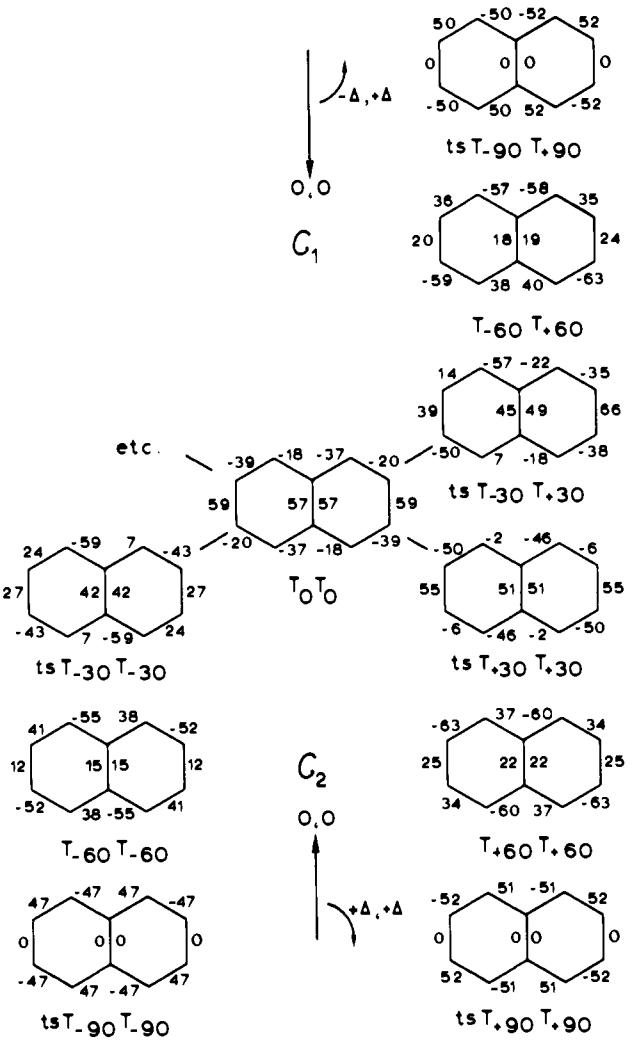

Figure 12. Torsion angles of the stable conformations and transition states on the C_1 and C_2 paths of twist–twist *cis*-decalin.

of 2.13 Å between the endo hydrogen atoms of the carbon atoms 2 and 6. In ts $T_{-30}T_{+30}$ there are short distances between the endo hydrogen atoms of the carbon atoms 4 and 5 (2.18 Å) and between the endo hydrogen atoms of the carbon atoms 1 and 6 (2.30 Å). The latter interaction can be likened to that of a methyl group on a flagpole position of boat cyclohexane. These short distances between the hydrogen atoms can easily be visualized from the inner drawings of Figure 5. This ends our description of the TT manifold. We have looked for direct links, other than T_0T_0, between the C_1 and C_2 paths, for instance transition states between $T_{+60}T_{+60}$ and $T_{-60}T_{+60}$, but unsuccessfully so far.

The ideal pseudorotation model thus turns out to be a useful guide to the flexible manifold of *cis*-decalin. The force field calculations corroborate the expected C_1 and C_2 pseudorotation paths. The six-membered rings are D_2 twistlike in the stable conformations and boatlike in the transition states. The deviations from the idealized geometries are minor, except for the highly strained transition states ts $T_{-30}T_{-30}$ and ts $T_{-30}T_{+30}$, and, of course, their isometric pseudorotation partners.

Chair–Twist to Twist–Twist Interconversion. The CT family has three stable conformations and six bonds in each chair ring that can be driven, in total 18 possible reaction paths for conversion to the TT manifold. Exploration of these 18 paths has yielded seven transition states; an eighth one is found from a brief inspection of the reverse process.[25] Continuous paths were not found in all cases. In general, a continuous reaction path is followed

(24) Allinger, N. L.; Coke, J. L. *J. Am. Chem. Soc.* **1959**, *81*, 4080–4082.

(25) Jensen and Beck[26] state that there are three different paths which appear to be of comparable energy but do not give the least information about the geometries involved.

(26) Jensen, F. R.; Beck, B. H. *Tetrahedron Lett.* **1966**, 4523–4528.

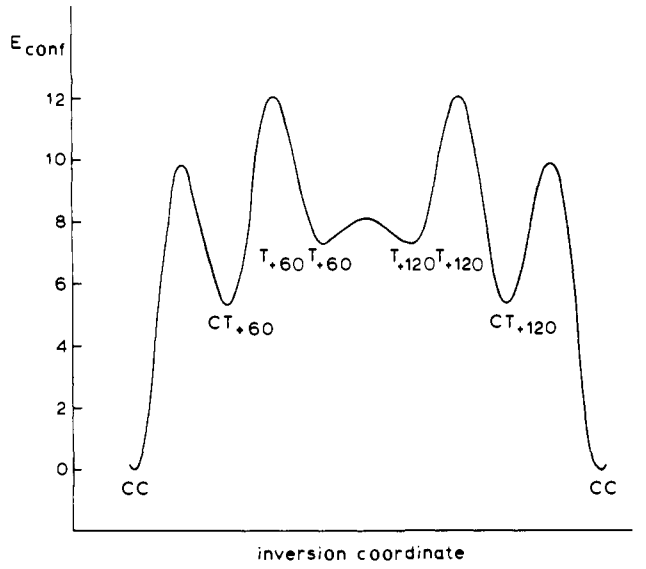

Figure 13. Conformational energy graph (kcal mol^{-1}) of the inversion of *cis*-decalin.

between the CT conformers and the transition states, but a movement perpendicular to the mapping parameters frequently occurs after the transition state has been passed. This results in a sudden decrease of the energy with a drastic reorganization of the geometry.[27] The conformational energies of the transition states range from 12.0 to 15.8 kcal mol^{-1} (Table I; for briefness' sake the intermediate [CT↔TT] will be omitted in the text of this section). Their geometries can be classified according to the phase angle of pseudorotation of ring A, which varies from −120 (ts1, ts2) via −60 (ts3, ts4), 0 (ts5, ts6), and +60 (ts7) to +120° (ts8). Efforts to locate a second transition state in the two latter cases were unsuccessful. Note that the transition states with a phase angle of pseudorotation of ring A over ±90° lead from CT forms with positively signed endocyclic torsion angles around the central bond to TT forms in which these torsion angles are negatively signed.

Special interest is attached naturally to the transition state of lowest energy, ts7, which was found by driving the mean of three torsion angles around bond 8–9 of CT_0 and CT_{+60} and around bond 7–8 of CT_{+60}. It connects the CT family to $T_{+60}T_{+60}$. A complete energy profile of the chair–chair inversion in *cis*-decalin can now be drawn (Figure 13). Two consecutive chair to twist conversions of the rings A and B bring the molecule from one CC form to $T_{+60}T_{+60}$; a pseudorotation over 60° along the C_2 path carries it to the enantiomer $T_{+120}T_{+120}$ from where it proceeds to the reversed enantiomeric CC form. The point of highest energy on this route (ts7) connects the most stable CT (and TC) conformer CT_{+60} to the most stable TT conformer $T_{+60}T_{+60}$. The calculated conformational energy of this transition state underestimates somewhat the experimental value (12.0 vs. 12.4 kcal mol^{-1}) which may be compared to the underestimation of the cyclohexane interconversion barrier[21] by the Engler force field (0.7 kcal mol^{-1}).

Geometrically, ts7 seems familiar (Figure 14): ring B looks like the transition state of cyclohexane with C_2 symmetry (three consecutive small torsion angles of the same sign with the driven torsion angle—the middle one—run well over zero), while ring A is about midway between boat and D_2 twist. The conformational energy of ts7 can be estimated from the experimental enthalpy of activation of the chair to twist transition state of cyclohexane[28] (10.8 kcal mol^{-1}) and the calculated strain of a form between D_2 twist and boat[21] (about 6.2 kcal mol^{-1}), after accounting for the

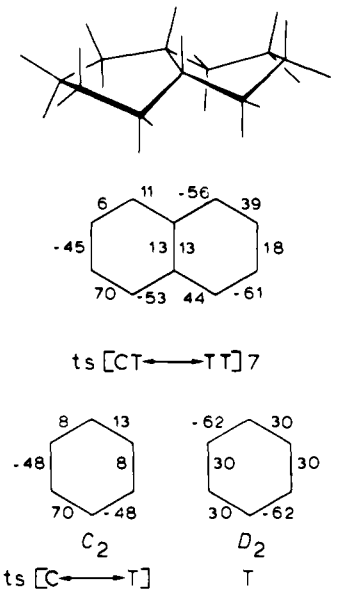

Figure 14. Comparison of ts[CT↔TT]7 with the C_2 transition state and the D_2 twist conformation of cyclohexane.

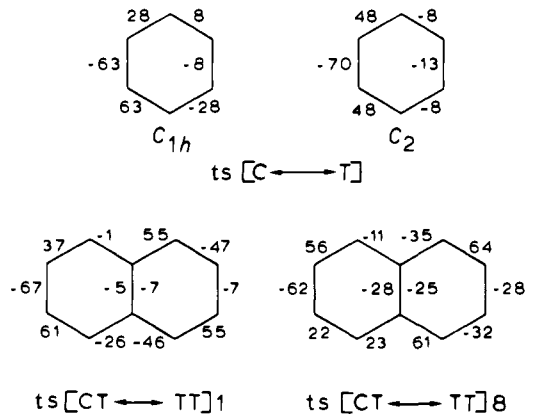

Figure 15. Comparison of ts[CT↔TT]1 and ts[CT↔TT]8 with the C_{1h} and C_2 transition states of cyclohexane.

loss of the ground-state strain of the cis fusion (see above, 2.7 kcal mol^{-1}) and the fact that the bicyclic system contains three almost eclipsed H–C–C–H units less than the constituent rings (at 13° about 2.5 kcal mol^{-1}). The net result of 10.8 + 6.2 − 2.7 − 2.5 = 11.8 kcal mol^{-1} is quite close to the experimental barrier of 12.4 kcal mol^{-1}.

The geometry of ts3 resembles that of ts7 closely as far as the converting ring is concerned. The twisted ring, however, differs considerably and has one of the methylene groups of the converting ring in a pseudo-axial, almost flagpole, position. This unfavorable feature explains the higher energy of this transition state. The next higher energy transition state with respect to ts7 is ts8. It has an unexpected geometry (Figure 15). Although ring A has an almost perfect D_2 twist conformation, the converting ring resembles neither the C_{1h} nor the C_2 cyclohexane transition state. The two torsion angles that have changed sign are both larger than 20°. The low energy of this curious and altogether unexpected transition state signals that one should be cautious in composing geometries of a complicated molecule using the structural data of its simpler constituents. Ts1 can be looked at as a combination of a boat and a C_{1h} cyclohexane transition state (Figure 15). Ts2 combines a ring A of similar geometry with a C_2 cyclohexane transition state but is of much higher energy. Finally, the transition states ts4-6 arise from converting the chair ring along the peripheral bonds. They are of much higher energy and need not be discussed further.

The high energy CC to TT transition state with a one step inversion along the central bond is saved from uninterest not only because of its aesthetic attractiveness but also because it has two

(27) Baas, J. M. A.; van de Graaf, B.; van Veen, A.; Wepster, B. M. *Recl. Trav. Chim. Pays-Bas* **1980**, *99*, 228–233.

(28) Anet, F. A. L.; Bourn, A. J. R. *J. Am. Chem. Soc.* **1967**, *89*, 760–768. Squillacote, M.; Sheridan, R. S.; Chapman, O. L.; Anet, F. A. L. *Ibid.* **1975**, *97*, 3244–3246.

imaginary frequencies. This shows that it is a two-dimensional saddle point (a transition state between transition states).

We compare finally the computed transition states with the literature proposals (see Figure 1). Neither the proposal of Gerig and Roberts[6] (G) nor that of De Pessemier, Anteunis, and Tavernier[7] (D) corresponds to the lowest transition state calculated here. Proposal G resembles best the high-energy transition states ts4-6. The geometry of proposal D is not too well reproduced in any of the computed transition states, but it is between ts7 and ts8, with the former one being the better approximation. Thus, the main idea of proposal D, a transition state with a small torsion angle around the central bond, is borne out by the computed transition states of lowest energy.

Acknowledgment. Professor Anteunis is thanked for his interest in this work.

Mechanism and Kinetic Characteristics of the Electrochemical Reduction of Carbon Dioxide in Media of Low Proton Availability

Christian Amatore and Jean-Michel Savéant*

Contribution from the Laboratoire d'Electrochimie de l'Université Paris 7, 75251 Paris Cedex 05, France. *Received January 28, 1981*

Abstract: The mechanism of the reduction of carbon dioxide in solvents of low proton availability such as dimethylformamide is investigated on the basis of the variation of the electrolysis product distribution with current density and concentration of CO_2 and water. It is shown to involve three competing pathways: oxalate formation through self-coupling of the $CO_2^{-}\cdot$ anion radicals, CO formation via oxygen–carbon coupling of $CO_2^{-}\cdot$ with CO_2, and formate formation through protonation of $CO_2^{-}\cdot$ by residual or added water followed by an homogeneous electron transfer from $CO_2^{-}\cdot$. Using the product distribution data together with the kinetic data obtained by fast microelectrolytic techniques allows the characterization of the key steps of the reduction process: initial electron transfer and the rate determining steps of the three competing reactions leading to oxalate, CO, and formate.

Carbon dioxide is an abundant and low-cost potential source of carbon for the production of fuels and organic chemicals. Electrochemical reduction provides a means of activating this particularly inert molecule. The nature of the reduction products crucially depends upon the reaction medium. In water, formic acid is the main product[1-4]

$$2CO_2 + H_2O + 2e^- \rightarrow HCO_2^- + HCO_3^-$$

while oxalate and carbon monoxide are obtained together with formate in solvents of low proton availability such as dimethylformamide, dimethyl sulfoxide, and propylene carbonate (see ref 3 and 5 and references cited therein).

$$2CO_2 + 2e^- \rightarrow C_2O_4^{2-}$$

$$2CO_2 + 2e^- \rightarrow CO + CO_3^{2-}$$

The addition of small amounts of water not only favors the formation of formate but also induces further reduction of oxalate, mainly into glycolate.[3,5]

Application of electrochemical[6] and spectroelectrochemical[7] microelectrolytic techniques, although providing some interesting thermodynamic and kinetic data, has not been able to give a description of the reaction mechanism and of the factors that determine the relative importance of the competing pathways leading to the various products. As made clear in the following, the distribution of products strongly depends upon operational factors such as current density, concentration, and diffusion layer thickness. This renders uncertain the extrapolation of results obtained in the context of microelectrolytic techniques to the conditions prevailing in macroscale electrolysis.

The discussion of the reaction mechanism and of the competition factors should thus mainly rely upon the determination of the distribution of products in preparative scale electrolysis and its systematic variations with the electrolysis parameters. This question has been addressed recently[5] leading to the proposal of the reaction mechanism depicted in Scheme I. However this scheme was developed on a qualitative basis, allowing no kinetic

Scheme I

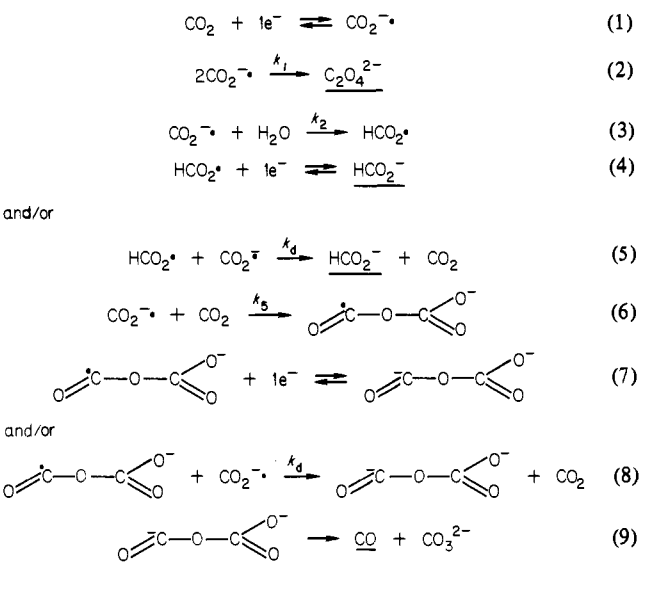

(1) Roberts, J. L.; Sawyer, D. T. *J. Electroanal. Chem.* **1965**, *9*, 1.
(2) Paik, N.; Andersen, T.; Eyring, H. *Electrochim. Acta* **1969**, *16*, 1217.
(3) Kaiser, V.; Heitz, E. *Ber. Bunsen. Gesell.*, **1973**, *77*, 818.
(4) Russel, P. G.; Novac, N.; Srinivasan, S.; Steinberg, M. *J. Electrochem. Soc.* **1977**, *124*, 1329.
(5) Gressin, J. C.; Michelet, D.; Nadjo, L.; Savéant, J.-M. *Nouv. J. Chim.* **1979**, *3*, 545.
(6) Lamy, E.; Nadjo, L.; Savéant, J.-M. *J. Electroanal. Chem.* **1977**, *78*, 403.
(7) Aylmer-Kelly, A. W. B.; Bewick, A.; Cantrill, P. R.; Tuxford, A. M. *Discuss. Faraday Soc.* **1973**, *56*, 96.

0002-7863/81/1503-5021$01.25/0